

Supporting information

ALD-made noble metal high entropy alloy nanofilm with sub-surface amorphization for enhanced hydrogen evolution

Yiming Zou, Lin Jing, Jianghong Zhang, Songzhu Luo, Leyan Wang, Yun Li, Ronn
Goei, Kwan W. Tan* and Alfred Iing Yoong Tok*

School of Materials Science and Engineering, Nanyang Technological University, 50
Nanyang Avenue, Singapore 639798, Singapore

*Corresponding authors: (K.W.T.) kwtan@ntu.edu.sg; (A.I.Y.T.) miytok@ntu.edu.sg.

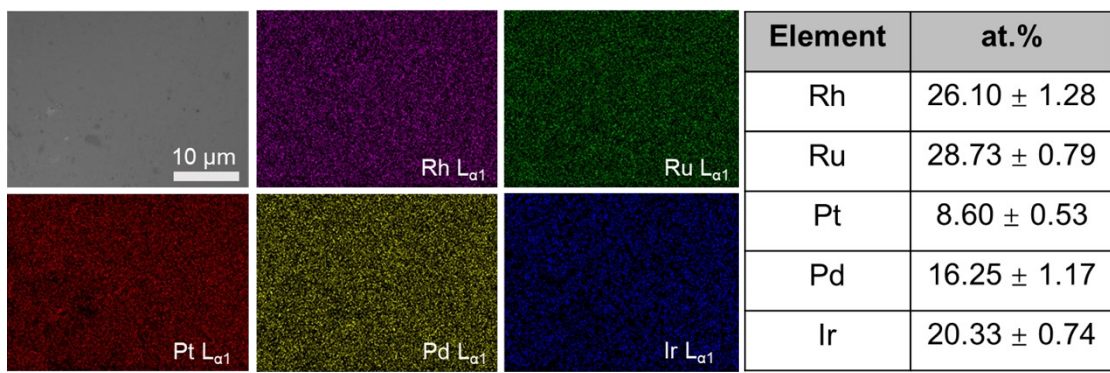


Fig. S1 Top-view EDX mappings of HEMG/GC and corresponding atomic concentrations of Rh, Ru, Pt, Pd, and Ir. All the noble metal elements are homogeneously distributed in the detected area.

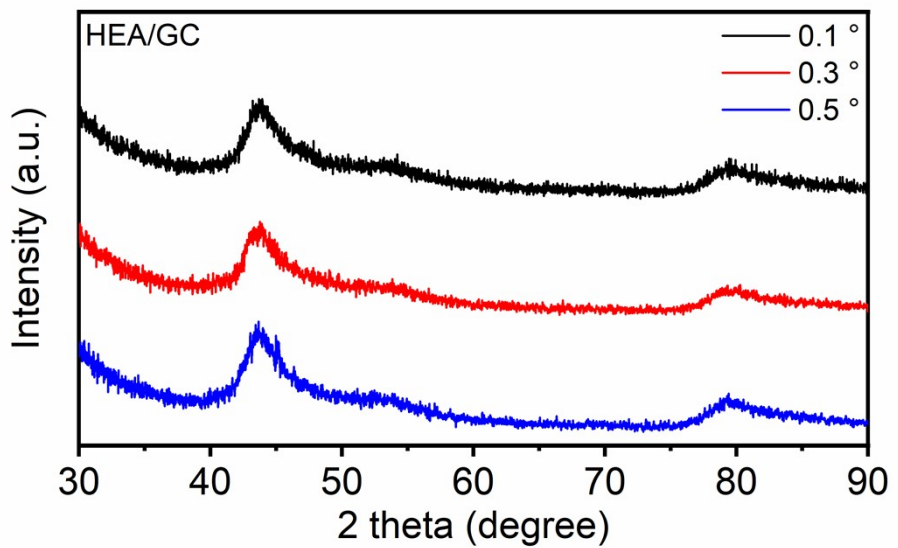


Fig. S2 GI-XRD patterns of HEMG/GC applied with 0.1, 0.3, and 0.5 ° incidence angles, respectively. No characteristic peak is shown other than peaks from glassy carbon substrates.

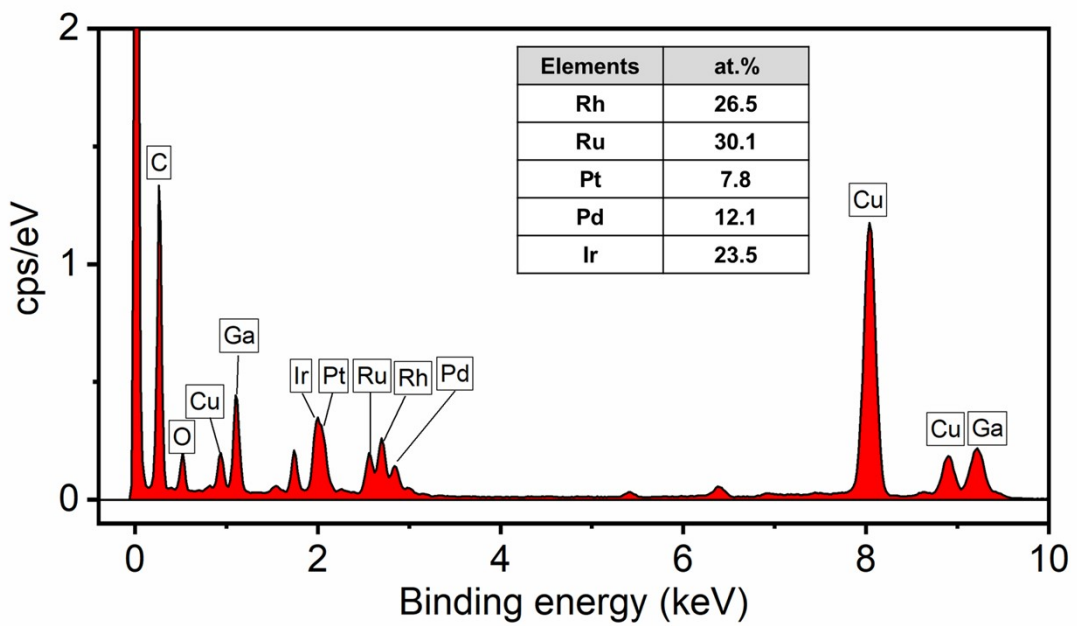


Fig. S3 EDX spectrum and corresponding atomic ratio of the cross section randomly selected from HEMG/GC. Cu signals are caused by the copper grid, and Ga signals are caused by Ga ion beam of FIB.

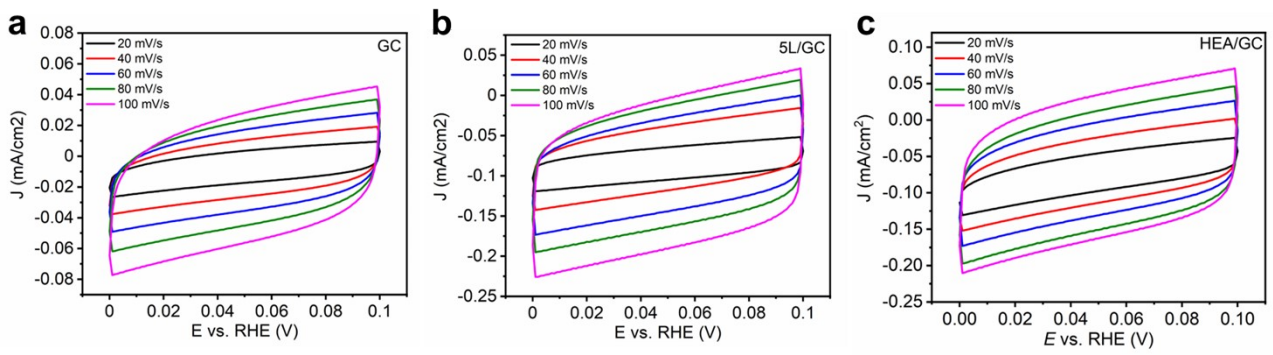


Fig. S4 CV curves of (a) GC, (b) 5L/GC, and (c) HEA/GC in a range of 0 to 0.1 V vs. RHE with scan rates of 20, 40, 60, 80, and 100 mV/s in 0.5 M H_2SO_4 .

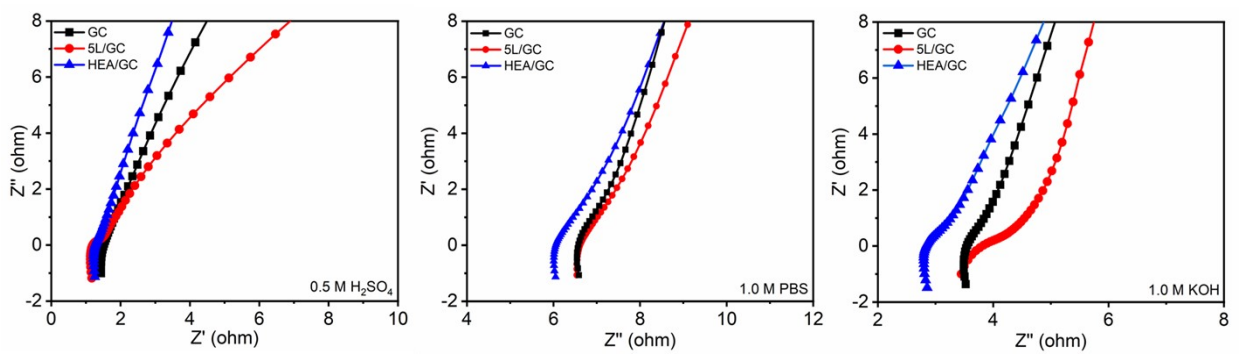


Fig. S5 EIS curves of GC, 5L/GC, and HEA/GC in (a) 0.5 M H_2SO_4 , (b) 1.0 M PBS, and (c) 1.0 M KOH.

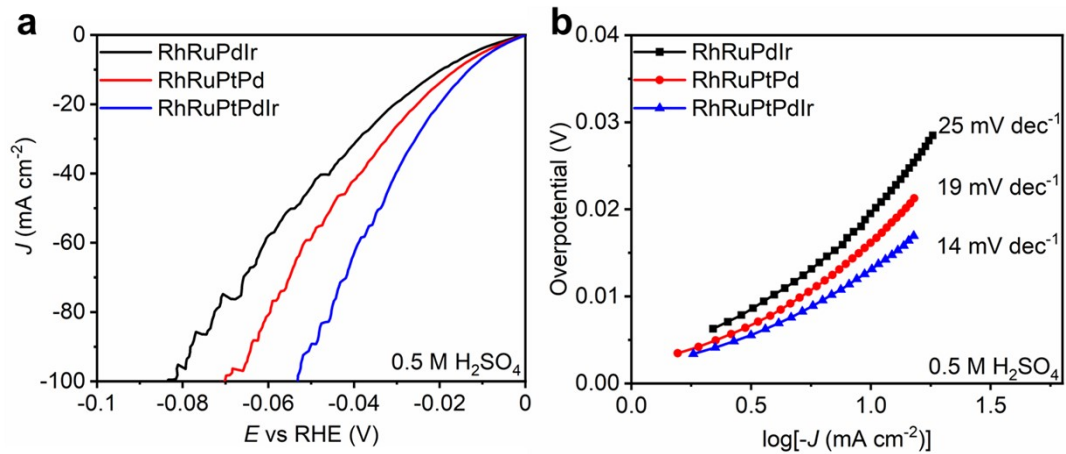


Fig. S6 The (a) LSV curves and (b) Tafel slopes of RhRuPdIr/GC, RhRuPdPt/GC, and RhRuPtPdIr/GC in 0.5 M H_2SO_4 .

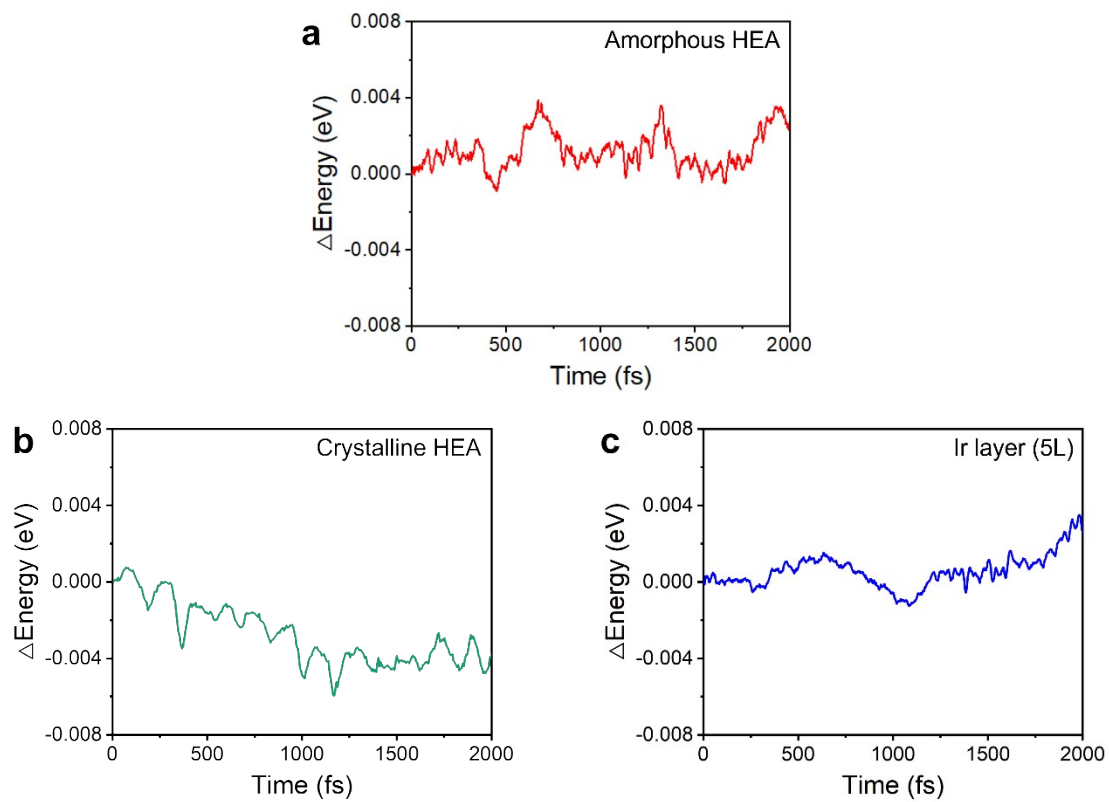


Fig. S7 Thermodynamic stability test by AIMD simulations. The energy change vs. time of (a) amorphous HEA, (b) crystalline HEA and (c) Ir layer (5L).

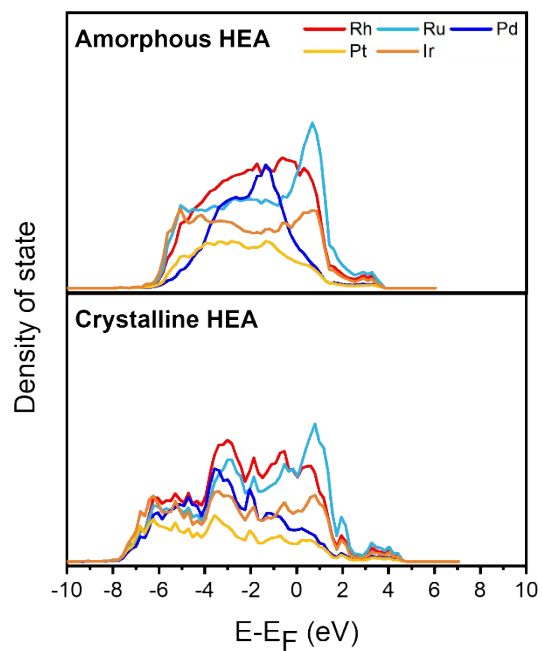


Fig. S8 PDOS of Rh, Ru, Pt, Pd, and Ir from (a) amorphous HEA and (b) crystalline HEA

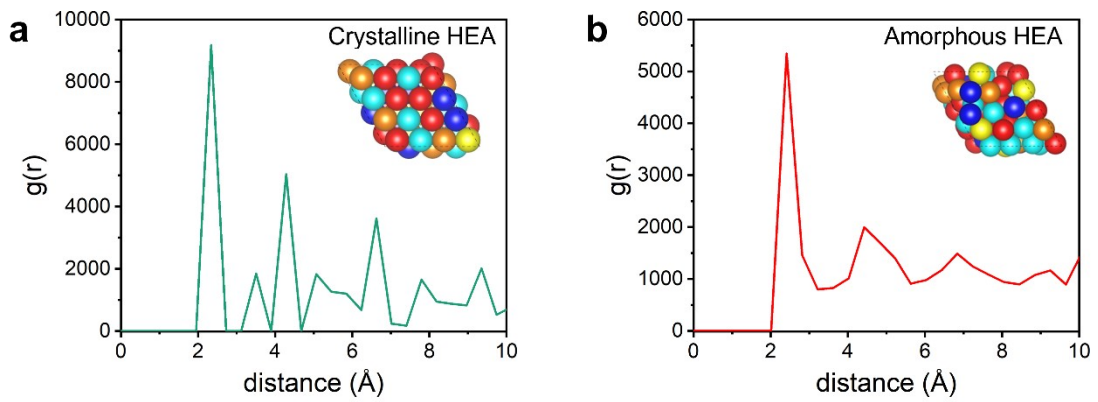


Fig. S9 Radial distribution function diagram of (a) crystalline HEA, (b) amorphous HEA (Inset: top view from [111] direction). The broader and smoother peaks exhibited by amorphous HEA indicates a transition from an ordered to a disordered structure.

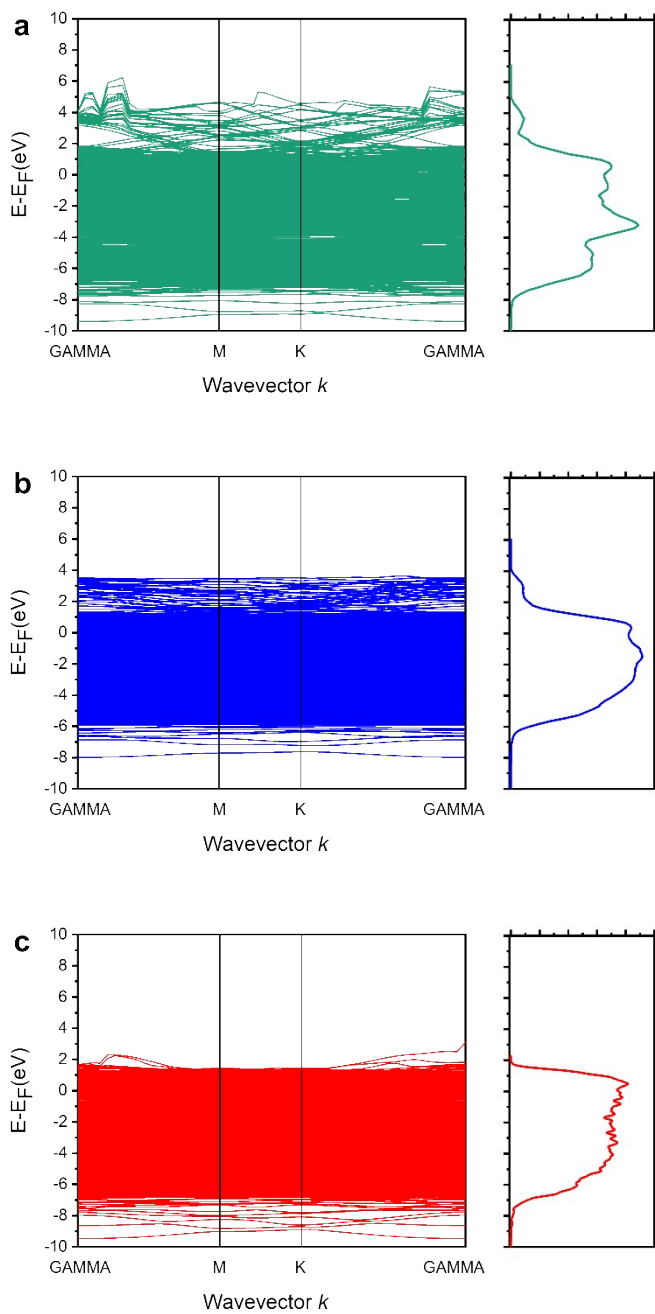


Fig. S10 Band structure of (a) crystalline HEA, (b) amorphous HEA and (c) Ir layer (5L).

Table S1 The binding energy of the major components identified in XPS spectra.

Elements	Bindings	Electrons	Binding energy (eV)
Rh	M-M	3d _{3/2}	312.0
		3d _{5/2}	307.2
	M-O	3d _{3/2}	312.9
		3d _{5/2}	308.1
Ru	M-M	3d _{3/2}	284.3
		3d _{5/2}	280.0
	M-O	3d _{3/2}	284.7
		3d _{5/2}	280.5
Pt	M-M	4f _{5/2}	74.5
		4f _{7/2}	71.2
		4d _{5/2}	315.0
	M-O	4f _{5/2}	75.4
		4f _{7/2}	72.1
Pd	M-M	3d _{3/2}	340.7
		3d _{5/2}	335.4
		2p _{3/2}	532.9
	M-O	3d _{3/2}	341.8
		3d _{5/2}	336.3
Ir	M-M	4f _{5/2}	63.7
		4f _{7/2}	60.7
		4d _{3/2}	313.2
	M-O	4f _{5/2}	64.5
		4f _{7/2}	61.4
C	C-C	1s	284.8
O	M-OH	1s	531.9
	M-O	1s	530.7
	C-O	1s	533.5

Table S2 Comparison of HER overpotential at 10 mA cm⁻² and Tafel slope in 0.5 M H₂SO₄ for best-performing noble-metal based catalysts.

Materials	Overpotential @ 10mA cm ⁻² (mV)	Tafel slope (mV dec ⁻¹)	Reference
RhRuPtPdIr	13	14	This work
Pt/C	40	30	1
Pd ₄₀ Ni ₁₀ Cu ₃₀ P ₂₀ MG	76	58	2
AlNiCoIrMo np	18.5	33.2	3
PdPtCuNiP MG	62	44.6	4
Np-UHEA14 (Al, Ag, Au, Co, Cu, Fe, Ir, Mo, Ni, Pd, Pt, Rh, Ru, and Ti)	32	30.1	5
Pt–CoP	52	28.2	6
Pt-Ru/CNT	12	23	7
Ru _{0.3} Pd _{0.7} @NPC	36	41	8
Cu/Rh(SAs) + Cu ₂ Rh(NPs)/GN)	8	24	9
Ni-MOF@Pt	43	30	10
K ₂ PtCl ₄ @NC-M	11	21	11

Table S3 Comparison of HER overpotential at 10 mA cm⁻² and Tafel slope in 1.0 M KOH for best-performing noble-metal based catalysts.

Materials	Overpotential @ 10mA cm ⁻² (mV)	Tafel slope (mV dec ⁻¹)	Reference
RhRuPtPdIr	66	78	This work
Ru/C ₃ N ₄ /C	79	69	12
PtNi	65	74	13
RuO ₂ /Co ₃ O ₄	89	91	14
Ru _{0.7} Pd _{0.3} @NPC	20	51	8
Ni-MOF@Pt	102	88	10
Ni ₃ N/Pt	50	36.5	15
PdFeCoNiCu/C	18	39	16
Pt ₁₈ Ni ₂₆ Fe ₁₅ Co ₁₄ Cu ₂₇ /C	11	30	17
Co-substitute Ru	13	29	18
Pt ₂₅ Pd ₂₅ Ni ₂₅ P ₂₅ MG	19.8	40	19
PdPtCuNiP MG	32	37.4	4
(FeCoNiB _{0.75}) ₉₇ Pt ₃	27	37.8	20

References

1. J.-S. Li, Y. Wang, C.-H. Liu, S.-L. Li, Y.-G. Wang, L.-Z. Dong, Z.-H. Dai, Y.-F. Li and Y.-Q. Lan, *Nat. Commun.*, 2016, **7**, 11204. <https://doi.org/10.1038/ncomms11204>.
2. Y. C. Hu, Y. Z. Wang, R. Su, C. R. Cao, F. Li, C. W. Sun, Y. Yang, P. F. Guan, D. W. Ding and Z. L. Wang, *Adv Mater*, 2016, **28**, 10293-10297. <https://doi.org/10.1002/adma.201603880>.
3. Z. Jin, J. Lv, H. Jia, W. Liu, H. Li, Z. Chen, X. Lin, G. Xie, X. Liu and S. Sun, *Small*, 2019, **15**, 1904180. <https://doi.org/10.1002/smll.201904180>.
4. Z. Jia, K. Nomoto, Q. Wang, C. Kong, L. Sun, L. C. Zhang, S. X. Liang, J. Lu and J. J. Kruzic, *Adv. Funct. Mater.*, 2021, **31**, 2101586. <https://doi.org/10.1002/adfm.202101586>.
5. Z.-X. Cai, H. Goou, Y. Ito, T. Tokunaga, M. Miyauchi, H. Abe and T. Fujita, *Chem. Sci.*, 2021, **12**, 11306-11315. <https://doi.org/10.1039/D1SC01981C>.
6. Y.-N. Zhou, X. Liu, C.-J. Yu, B. Dong, G.-Q. Han, H.-J. Liu, R.-Q. Lv, B. Liu and Y.-M. Chai, *J. Mater. Chem. A*, 2023, **11**, 6945-6951. <https://doi.org/10.1039/D2TA09784B>.
7. D. Zhang, Z. Wang, X. Wu, Y. Shi, N. Nie, H. Zhao, H. Miao, X. Chen, S. Li and J. Lai, *Small*, 2022, **18**, 2104559. <https://doi.org/10.1002/smll.202104559>.
8. J. Huang, C. Du, Q. Dai, X. Zhang, J. Tang, B. Wang, H. Zhou, Q. Shen and J. Chen, *J. Alloys Compd.*, 2022, **917**, 165447. <https://doi.org/10.1016/j.jallcom.2022.165447>.
9. S. Sultan, M. H. Diorizky, M. Ha, J. N. Tiwari, H. Choi, N. K. Dang, P. Thangavel, J. H. Lee, H. Y. Jeong and H. S. Shin, *J. Mater. Chem. A*, 2021, **9**, 10326-10334. <https://doi.org/10.1039/D1TA01067K>.
10. K. Rui, G. Zhao, M. Lao, P. Cui, X. Zheng, X. Zheng, J. Zhu, W. Huang, S. X. Dou and W. Sun, *Nano Lett.*, 2019, **19**, 8447-8453. <https://doi.org/10.1021/acs.nanolett.9b02729>.
11. H. Jin, S. Sultan, M. Ha, J. N. Tiwari, M. G. Kim and K. S. Kim, *Adv. Funct. Mater.*, 2020, **30**, 2000531. <https://doi.org/10.1002/adfm.202000531>.
12. Y. Zheng, Y. Jiao, Y. Zhu, L. H. Li, Y. Han, Y. Chen, M. Jaroniec and S.-Z. Qiao, *J. Am. Chem. Soc.*, 2016, **138**, 16174-16181. <https://doi.org/10.1021/jacs.6b11291>.
13. Z. Cao, Q. Chen, J. Zhang, H. Li, Y. Jiang, S. Shen, G. Fu, B.-a. Lu, Z. Xie and L. Zheng, *Nat. Commun.*, 2017, **8**, 15131. <https://doi.org/10.1038/ncomms15131>.
14. N. Wu, C. Liu, D. Xu, J. Liu, W. Liu, H. Liu, J. Zhang, W. Xie and Z. Guo, *J. Mater. Chem. C*, 2019, **7**, 1659-1669. <https://doi.org/10.1039/C8TC04984J>.
15. Y. Wang, L. Chen, X. Yu, Y. Wang and G. Zheng, *Adv. Energy Mater.*, 2017, **7**, 1601390. <https://doi.org/10.1002/aenm.201601390>.
16. D. Zhang, Y. Shi, H. Zhao, W. Qi, X. Chen, T. Zhan, S. Li, B. Yang, M. Sun and J. Lai, *J. Mater. Chem. A*, 2021, **9**, 889-893. <https://doi.org/10.1039/D0TA10574K>.
17. H. Li, Y. Han, H. Zhao, W. Qi, D. Zhang, Y. Yu, W. Cai, S. Li, J. Lai and B. Huang, *Nat. Commun.*, 2020, **11**, 5437. <https://doi.org/10.1038/s41467-020-19277-9>.
18. J. Mao, C.-T. He, J. Pei, W. Chen, D. He, Y. He, Z. Zhuang, C. Chen, Q. Peng, D. Wang and Y. Li, *Nat. Commun.*, 2018, **9**, 4958. <https://doi.org/10.1038/s41467-018-07288-6>.
19. Z. Jia, Y. Yang, Q. Wang, C. Kong, Y. Yao, Q. Wang, L. Sun, B. Shen and J. J. Kruzic, *ACS Mater. Lett.*, 2022, **4**, 1389-1396. <https://doi.org/10.1021/acsmaterialslett.2c00371>.
20. X. Zhang, Y. Yang, Y. Liu, Z. Jia, Q. Wang, L. Sun, L. C. Zhang, J. J. Kruzic, J. Lu and B. Shen, *Adv Mater*, 2023, 2303439. <https://doi.org/10.1002/adma.202303439>.